Supplementary Information for

Sensitivity of Gas Sensors Enhanced by Functionalization of Hexabenzoperylene in Solution-Processed Monolayer Organic Field Effect Transistors

Qi Gong, Qian Miao*

Department of Chemistry, The Chinese University of Hong Kong, Shatin, Hong Kong

* email: miaoqian@cuhk.edu.hk

Table of Contents

1. Synthesis

General: The reagents and starting materials employed were commercially available and used without any further purification or prepared following reported methods as indicated. Anhydrous and O_2-free diethyl ether, THF, CH_2Cl_2 and toluene were obtained from an Advanced Technology Pure-Solv PS-MD-4 system. NMR spectra were recorded on a Bruker AVANCE III 400MHz spectrometer (1H NMR: 400 MHz, 13C NMR: 100 MHz). Chemical shift values (δ) are expressed in parts per million using residual solvent protons (^{1}H NMR, δ(H) is 7.26 ppm for $CDCl_3$, ^{13}C NMR, δ(C) is 77.16 for $CDCl_3$, δ(C) is 73.78 for C2D2Cl4) as internal standard. Mass spectra were recorded on a Therno Finnigan MAT 95 XL spectrometer. Melting points, without correction, were measured using a Nikon Polarized Light Microscope ECLIPSE 50i POL equipped with an INTEC HCS302 heating stage.

Hexabenzoperylenes (HBPs) **1** and **2** and 12-methoxylphosphonic acid (MODPA) were synthesized following the reported procedures. [1, 2, 3]

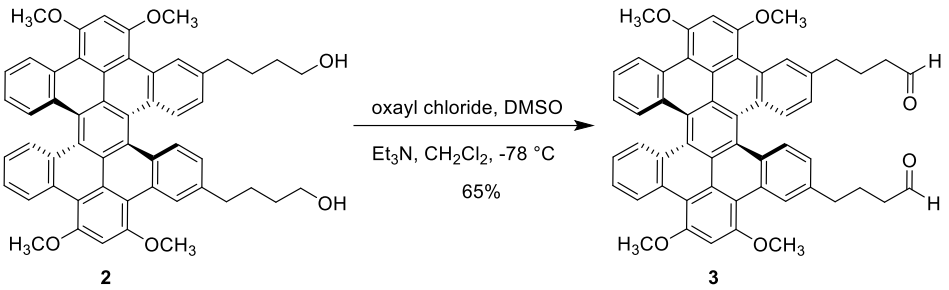

Scheme S1 Synthesis of **3**.

4,4'-(9,11,20,22-tetramethoxyhexabenzo[*a,cd,f,j,lm,o*]perylene-2,7-diyl)bis(butan-1-al) (**3**)

To a stirred solution of oxayl chloride (0.25 mL, 3 mmol) in 20 mL dry CH_2Cl_2 at -78 ℃ was added dimethyl sulfoxide (0.4 mL, 5.6 mmol). The solution was stirred for 15 min. A suspension of **2** (50 mg, 0.063 mmol) in 10 mL of dry CH_2Cl_2 was added into the solution, which was then stirred for 50 min. The reaction mixture was treated with triethylamine (1 mL, 7.2 mmol) and allowed to warm to room temperature and react for 1.5 h. The resulting mixture was washed with water and extracted with CH_2Cl_2 (3 × 20 mL). The resulting solution was concentrated under reduced pressure, and the residue was purified by column chromatography on silica gel using CH_2Cl_2 as eluent to afford compound **3** in a yield of 65%. mp: over 350℃. ^{1}HNMR ($CDCl_3$) δ (ppm): 9.79 (s, 2H), 9.45 (d, J_2 = 8.0 Hz, 2H), 9.24 (s, 2H), 8.55 (m, 4H), 7.44 (m, 4H), 7.17 (t, J_3 = 7.6 Hz, 2H), 7.00 (d, J_2 = 8.4 Hz, 2H), 4.34 (s, 12H), 2.84 (t, J_3 = 7.2 Hz, 4H), 2.53 (t, J_3 = 6.8 Hz), 2.11 (m, 4H); ^{13}C NMR ($CDCl_3$) δ (ppm): 202.7, 158.1, 158.0, 139.2, 131.1, 131.0, 129.6, 129.0, 128.9, 127.7, 127.2, 126.5, 126.4, 126.0, 125.4, 125.3, 124.2, 113.7, 113.6, 97.2, 56.6, 56.5, 43.3, 35.6, 23.7; MS (APCI$^+$): $[M+H]^+$ calculated for $C_{54}H_{42}O_6$, 787.3048; found:787.3054..

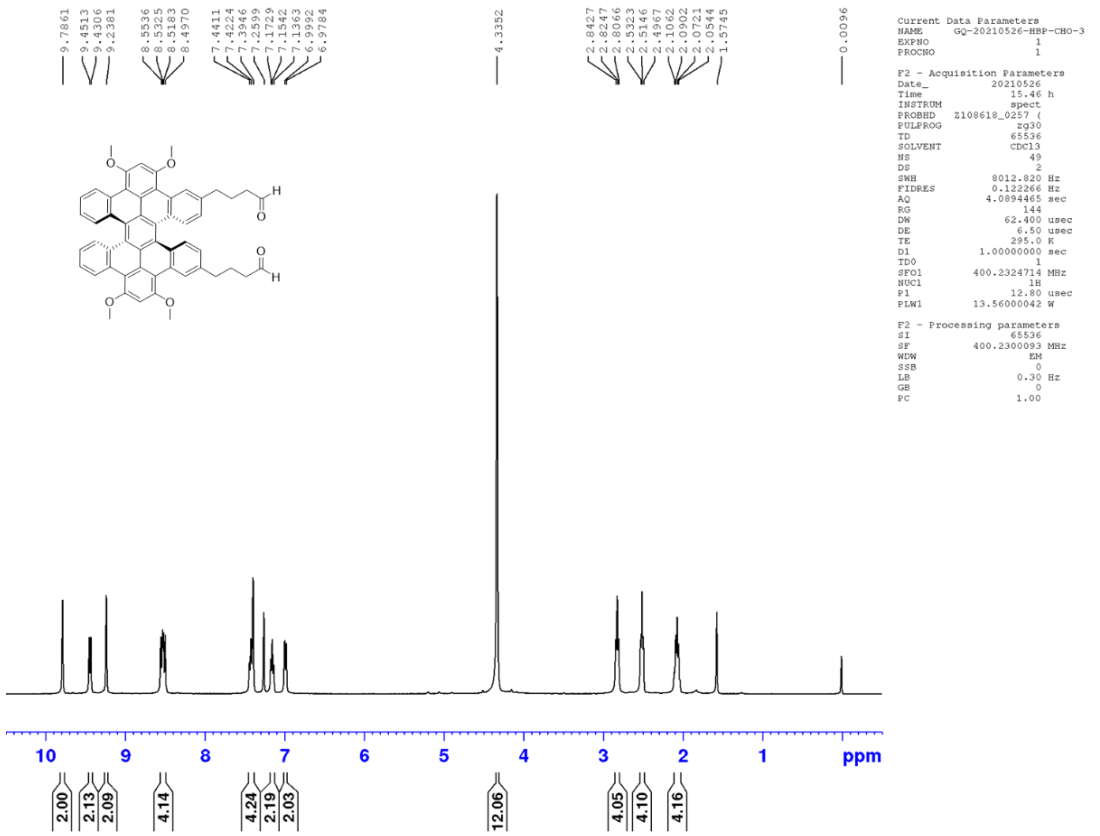

Figure S1 ^{1}H NMR of compound **3** ($CDCl_3$)

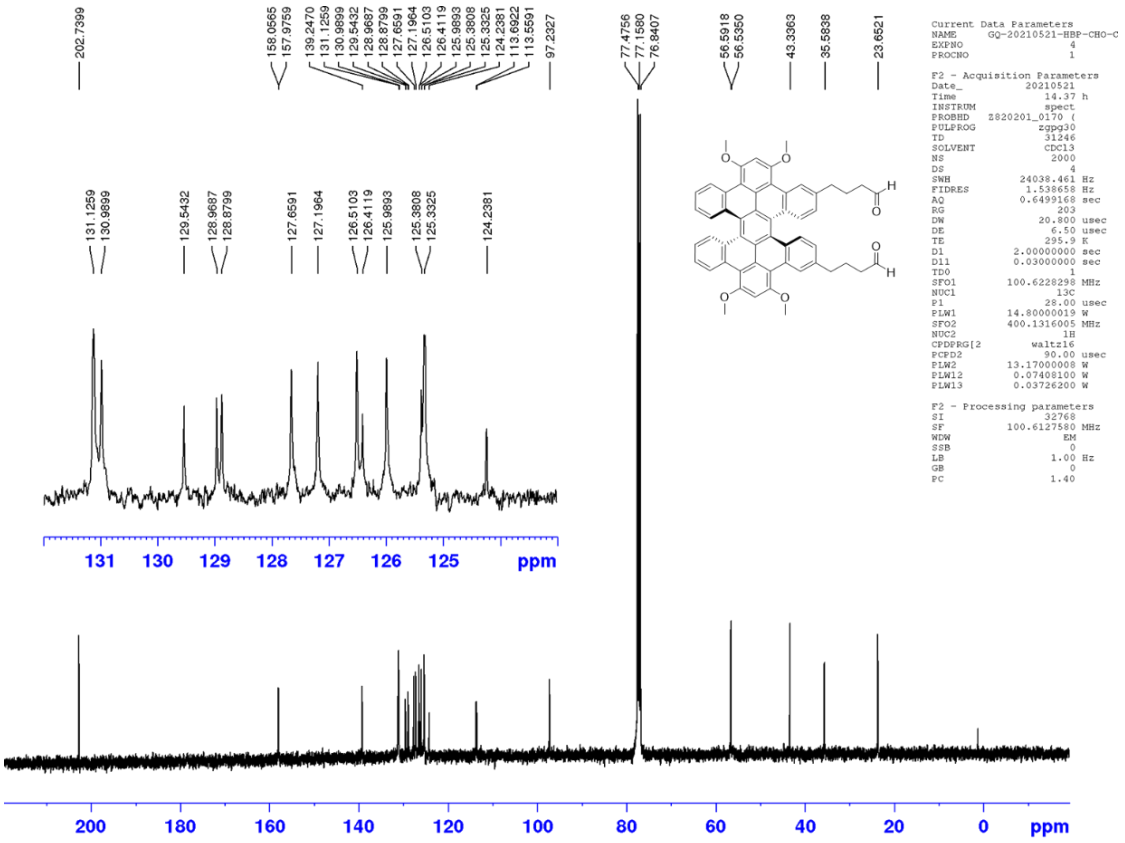

Figure S2 ^{13}C NMR of compound **3** ($CDCl_3$)

2. Cyclic voltammetry

Cyclic voltammetry was performed on a PAR Potentiostat /Galvanostat Model 263A Electrochemical Station (Princeton Applied Research) at a scan rate of 50 $mV \cdot s^{-1}$. Compound **3** was dissolved in anhydrous CH_2Cl_2 that contained 0.1 M of tetrabutylammonium hexafluorophosphate (Bu4NPF6) as supporting electrolyte. A platinum bead was used as a working electrode, a platinum wire was used as an auxiliary electrode, and a silver wire was used as a pseudo-reference. Cobaltocene/cobaltocenium was used as an internal standard. Potentials were referenced to ferrocenium/ferrocene ($FeCp_2^+/FeCp_2^0$).

Table S1 Summary of electrochemical potentials and energy levels of HOMO

Compound	E_{ox}^1 (V)[a]	E_{ox}^2 (V)[a]	HOMO (eV)[b]
3	0.25	0.53	−5.35

a. Half-wave potential versus $FeCp_2^+/FeCp_2^0$, b. Estimated from HOMO = −5.10 – E_{ox}^1 (eV).[4]

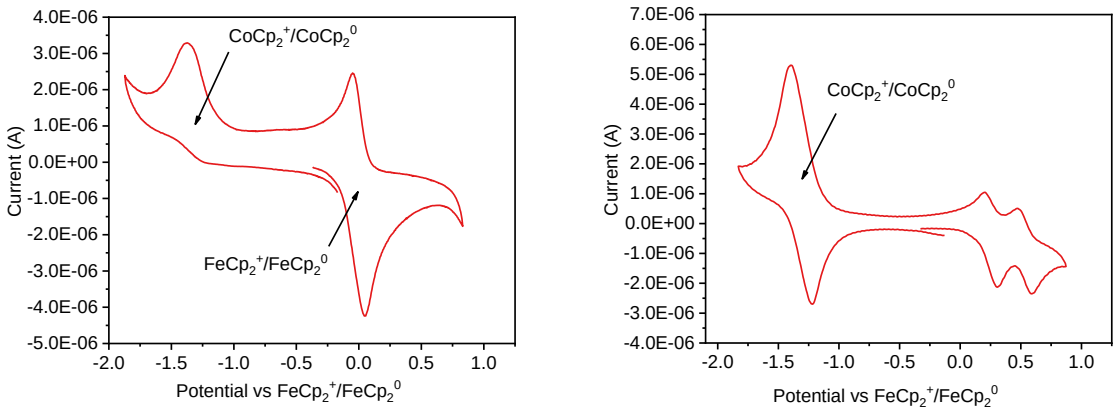

Figure S3 Cyclic voltammograms of **3**.

3. Fabrication and Characterization of Thin Films and Organic Field Effect Transistors

MODPA-modified $AlO_x/TiO_y/Si$ dielectric was prepared following the reported procedure.[3] Thin films of **1**, **2**, **3** and their mixtures of the indicated mass ratios were formed by immersing the substrate into the corresponding solution (1 mg/mL) in a mixed solvent and then pull it up with a constant speed using a LongerPump TJ-3A syringe pump. The solvents and pulling speeds are shown in Table S2, S3 and S6. The dip-coated films were placed in vacuum at room temperature for 3 h to remove the solvent residue. For fabrication of organic field effect transistors (OFETs), top contact drain and source gold electrodes (30 nm) were vacuum-deposited through a shadow mask onto the organic films using an Edward Auto 306 vacuum coating system with a Turbomolecular pump at a pressure of 4.0×10^{-6} torr or lower, with a deposition rate of ca. 2 nm/min to a thickness about 30 nm as measured by a quartz crystal sensor. The resulting semiconducting channels were 1 mm (W)×50 μm (L). The field effect mobility in the saturation regime was extracted from these curves using the equation: $I_{DS} = (\mu WC_i/2L)(V_{GS}-V_{th})^2$, where I_{DS} is the drain current, μ is field effect mobility, C_i (= 24 ±0.6 nF/cm^2) is the capacitance per unit area for the MODPA-modified AlO_x/TiO_y,[2] W is the channel width, L is the channel length, and V_{GS} and V_{th} are the gate and threshold voltage, respectively.

Polarized light micrographs were obtained using a Nikon 50IPOL microscope. Atomic force microscopy (AFM) topographic images were obtained using a Bruker Dimension Icon system using tapping mode in air under ambient conditions. X-ray diffractions from thin films were recorded with a SmartLab X-Ray Refractometer. Contact angle measurement was conducted using an optical contact angle meter (OCA25, Dataphysics, Germany) with oscillating drop accessory ODG-20 (Dataphysics Instruments GmbH, Germany). Current-voltage measurement of OFETs was conducted using a probe station and a Keithley 4200 Semiconductor Characterization System in air under ambient conditions.

(1) Monolayer films and OFETs of **1**.

Table S2 Summary of the dip-coated monolayer films of **1** on MODPA-modified $AlO_x/TiO_y/Si$.

Solvent	Speed (um/min)	Thickness (nm)	Mobility (cm^2/Vs)
CH_2Cl_2 / Ethyl Acetate 1:1	1.5	2.5~2.7	0.010 ± 0.006

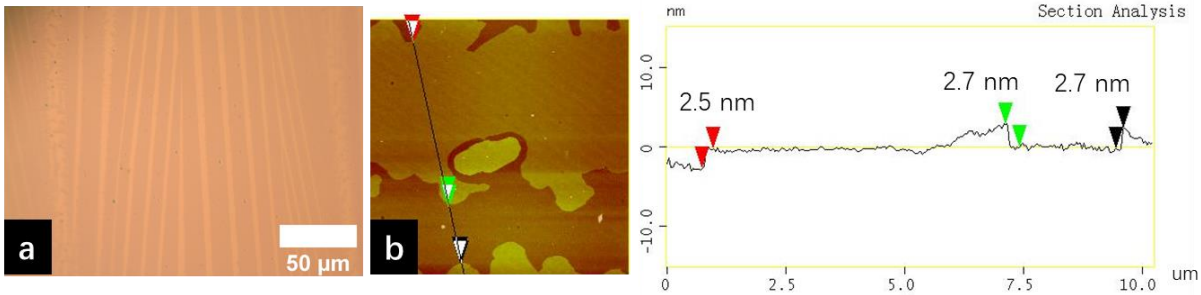

Figure S4 (a) Reflection polarized light micrograph from dip coating monolayer film of **1** on MODPA-modified $AlO_x/TiO_y/Si$. (b)AFM cross-section analysis for monolayer film of **1** on MODPA-modified $AlO_x/TiO_y/Si$.

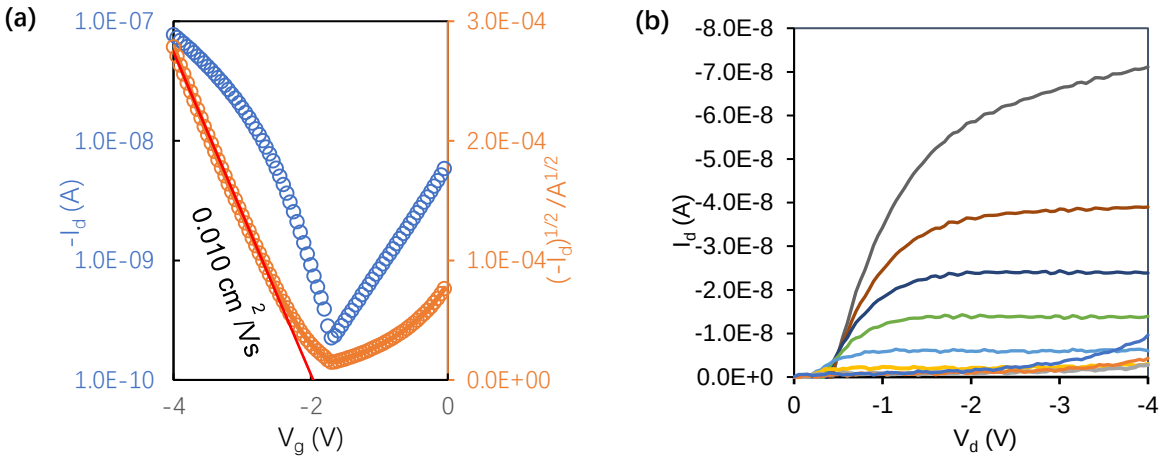

Figure S5 (a) Transfer I-V curves of a typical monolayer OFET of **1** with a channel of 50 μm (L)×1 mm (W) as tested in air; (b) output curves of the same OFET of **1** with gate voltage varied from 0 to −4V in −0.5 V steps.

(2) Films and OFETs of **2** and **1&2**

Table S3 Summary of dip coating films of **2** and **1&2** (with the mass ratio shown in the bracket) on MODPA-modified AlO_x/TiO_y/Si.

Film	**2**	**1&2** (1:1)	**1&2** (2:1)	**1&2** (5:1)	**1&2** (10:1)
Solvent	CH_2Cl_2/acetone=1:1	CH_2Cl_2 / ethyl acetate = 1:1			
Pulling speed	1 mm/min				
Thickness (nm)	10~20	1.7~3.9	1.9~2.0	2.4~2.5	3.7~5.9
Mobility (cm^2/Vs)	$(3.2\pm1.0)\times10^{-3}$	$(4.9\pm2.1)\times10^{-4}$	$(6.0\pm1.9)\times10^{-4}$	$(5.0\pm2.2)\times10^{-3}$	$(4.9\pm3.1)\times10^{-3}$

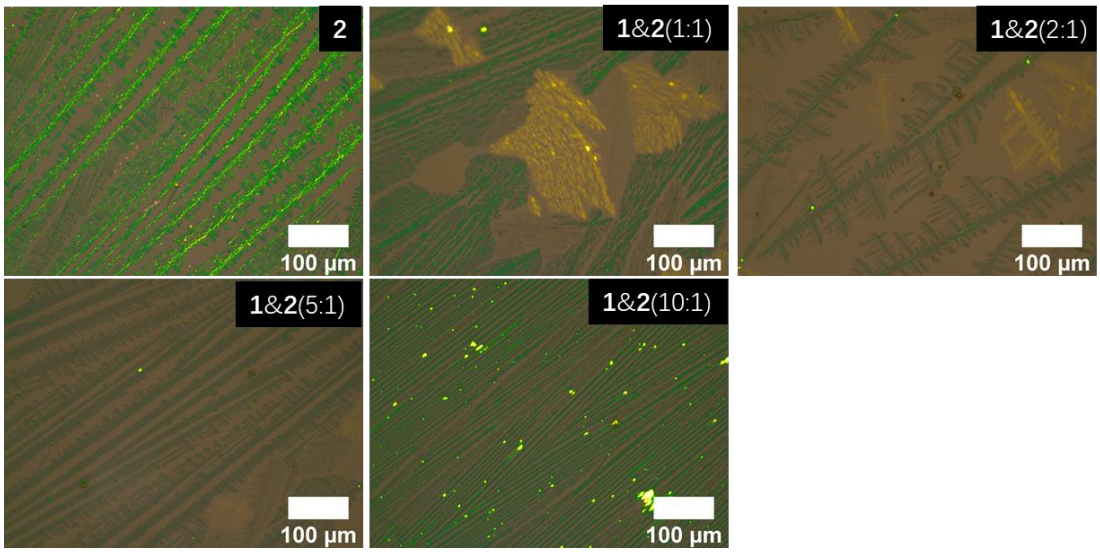

Figure S6 Reflection polarized light micrographs of dip-coated films of **1** and **2** on MODPA-modified $AlO_x/TiO_y/Si$.

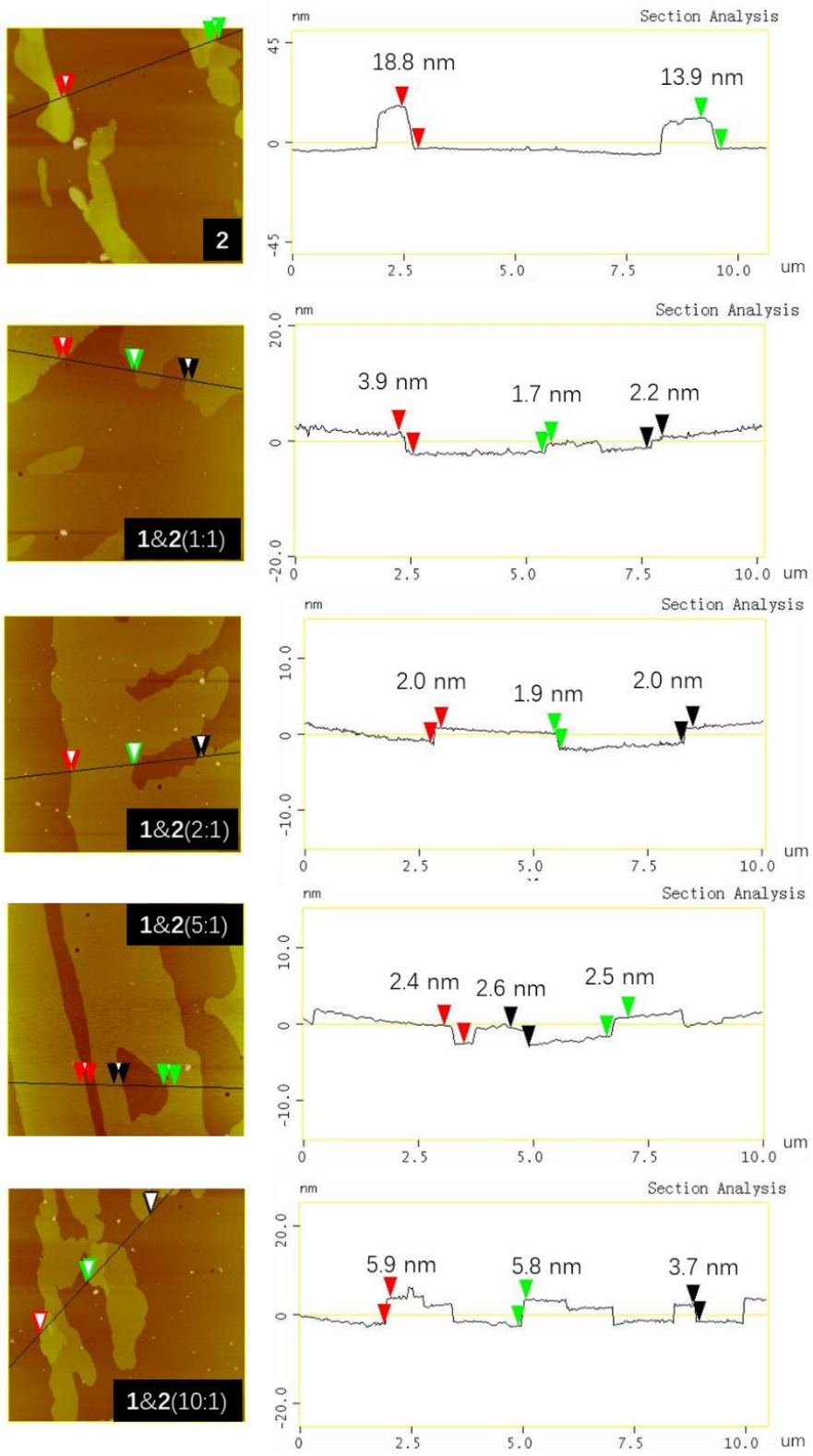

Figure S7 AFM images and cross-section analysis for films of **2** and **1&2** on MODPA-modified $AlO_x/TiO_y/Si$.

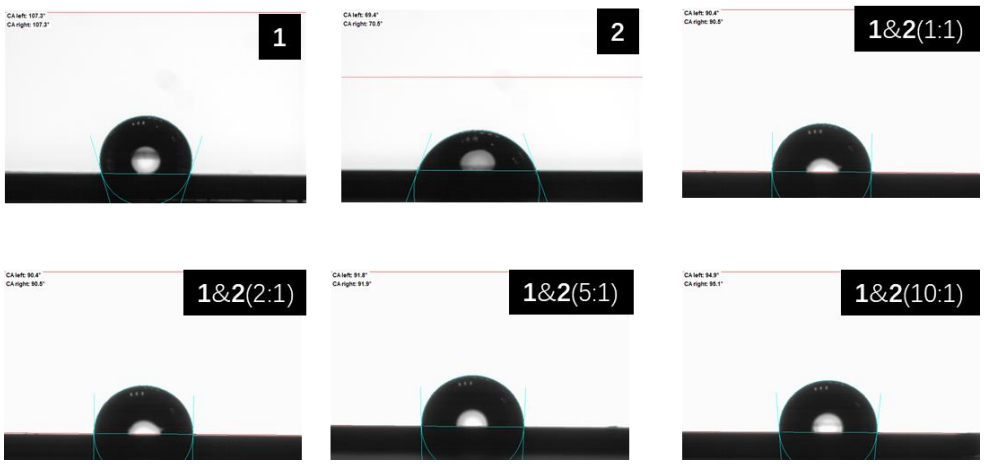

Figure S8 Measurement of the contact angle of the dip-coated films of **1**, **2** and **1&2** with one drop of deionized water.

Table S4 Static contact angles of the dip-coated films of **1**, **2** and **1&2** with deionized water.

1	**2**	**1&2**(1:1)	**1&2**(2:1)	**1&2**(5:1)	**1&2**(10:1)
107.9°	70.5°	90.7°	91.5°	93.4°	95.1°

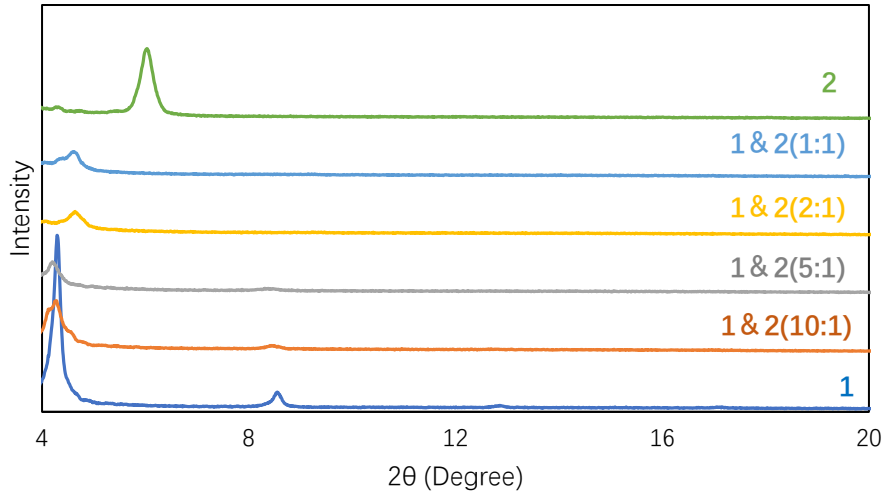

Figure S9 XRD patterns of dip-coated films of **1**, **2** and **1&2** on the MODPA-modified AlO_x TiO_y/Si.

Table S5 Summary of X-ray diffraction patterns of dip-coated films of **1**, **2** and **1&2** on the MODPA-modified AlO_x TiO_y/Si.

Film	2θ (Degree)	d (nm)
1	4.29	2.06
1&2 (10:1)	4.28	2.06
1&2 (5:1)	4.20	2.10
1&2 (2:1)	4.62	1.91
1&2 (1:1)	4.64	1.90
2	6.03	1.47

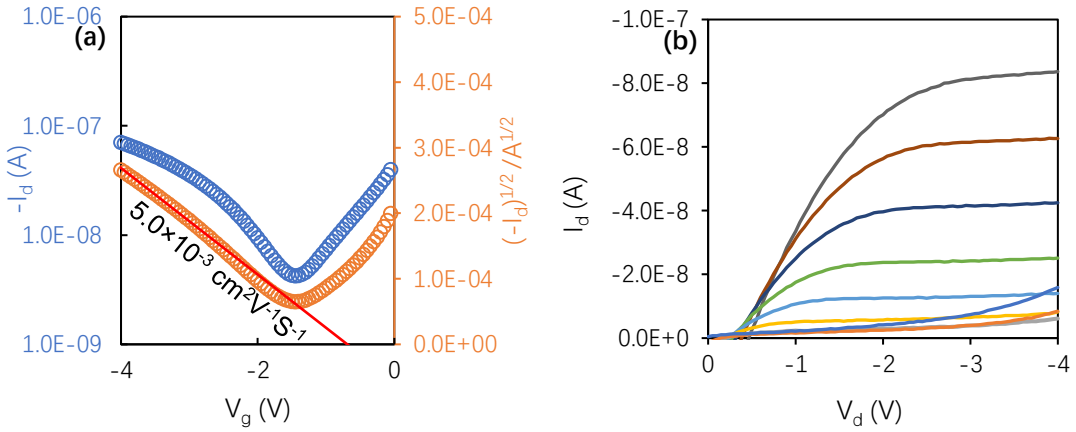

Figure S10 (a) Transfer I-V curves of a typical OFET of **1&2** (5:1) with a channel of 50 μm (L)×1 mm (W) as tested in air; (b) output I-V curves of the same OFET of **1&2** (5:1) with the gate voltage varied from 0 to −4V in −0.5 V steps.

(3) Films and OFETs of **3** and **1&3**.

Table S6 Summary of dip-coated films of **3** and **1&3** (with the mass ratio shown in the bracket) on MODPA-modified AlO_x/TiO_y/Si.

Film	**3**	**1&3** (1:2)	**1&3** (1:1)	**1&3** (5:1)
solvent	CH_2Cl_2/Hexane=1:1	CH_2Cl_2 / ethyl acetate = 1:1		
Pulling speed	1 mm/min			
Thickness (nm)	6.2~10	1.8~5.6	1.8~2.3	1.9~2.0
Mobility (cm^2/Vs)	$(3.2\pm1.3)\times10^{-3}$	$(6.0\pm2.4)\times10^{-4}$	$(5.9\pm2.3)\times10^{-4}$	$(5.0\pm2.6)\times10^{-3}$

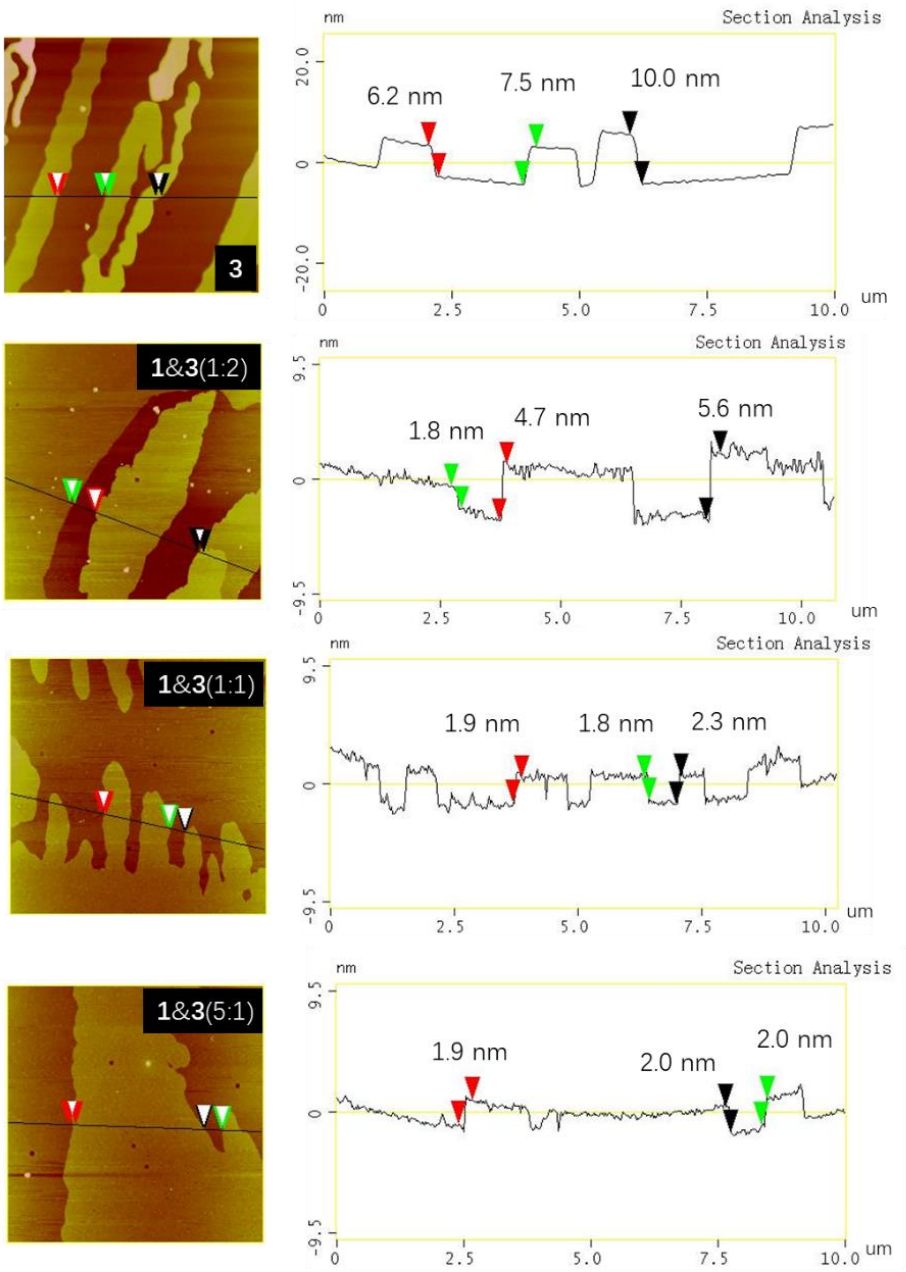

Figure S11 AFM cross-section analysis for films of **1** and **3** on MODPA-modified $AlO_x/TiO_y/Si$.

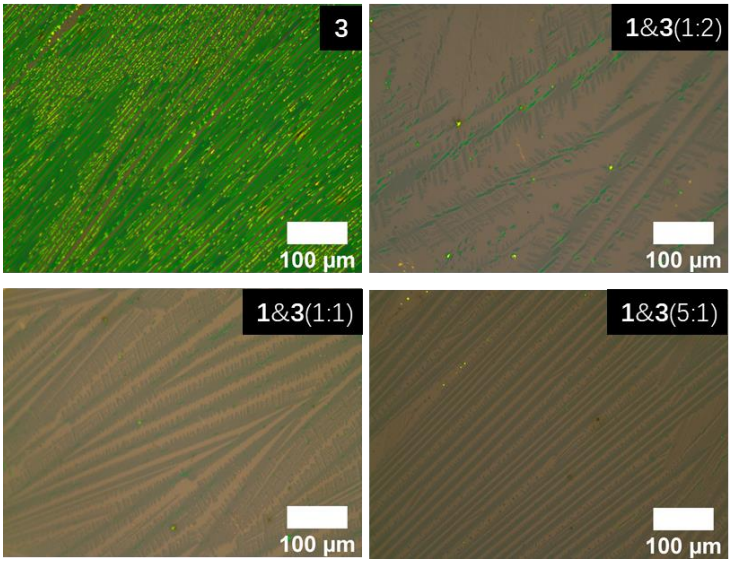

Figure S12 Reflection polarized light micrographs of dip-coated films of **3** and **1&3** on MODPA-modified $AlO_x/TiO_y/Si$.

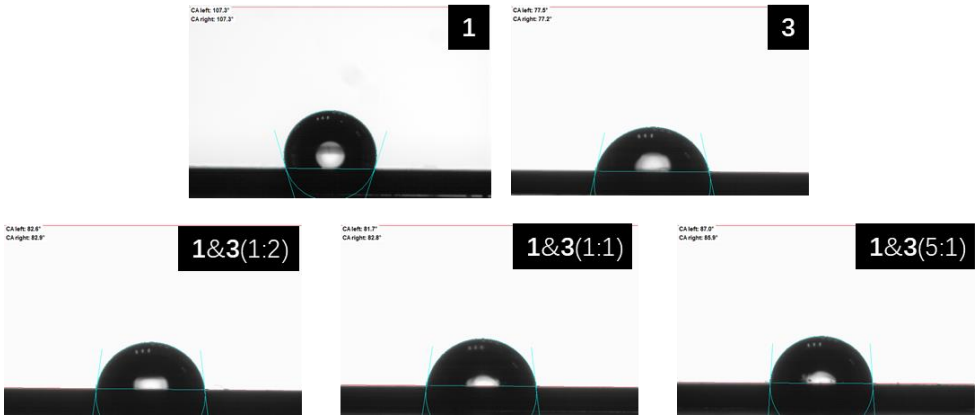

Figure S13 Measurement of contact angle of the dip-coated films of **1**, **3**, and **1&3** with one drop of deionized water.

Table S7 Static contact angles of the dip-coated films of **1**, **3** and **1&3** with deionized water.

1	**3**	**1&3**(1:2)	**1&3**(1:1)	**1&3**(5:1)
107.9°	77°	82°	82.4°	87.6°

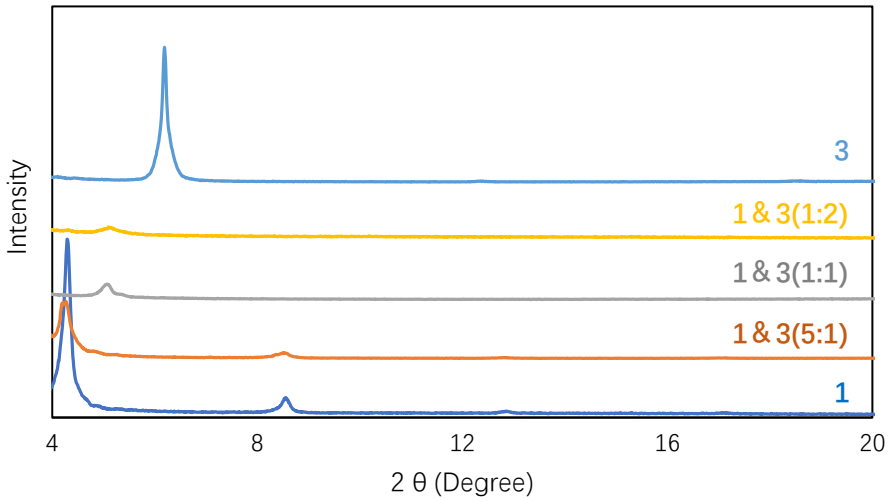

Figure S14 XRD patterns of dip-coated films of **1**, **3** and **1&3** on the MODPA /AlOx TiO_y/Si.

Table S8 Summary of the XRD patterns of dip-coated films of **1**, **3** and **1&3** on the MODPA /AlOx TiO_y/Si.

Film	2θ (Degree)	d (nm)
1	4.29	2.06
1&3(5:1)	4.27	2.07
1&3(1:1)	5.08	1.74
1&3(2:1)	5.1	1.73
3	6.19	1.43

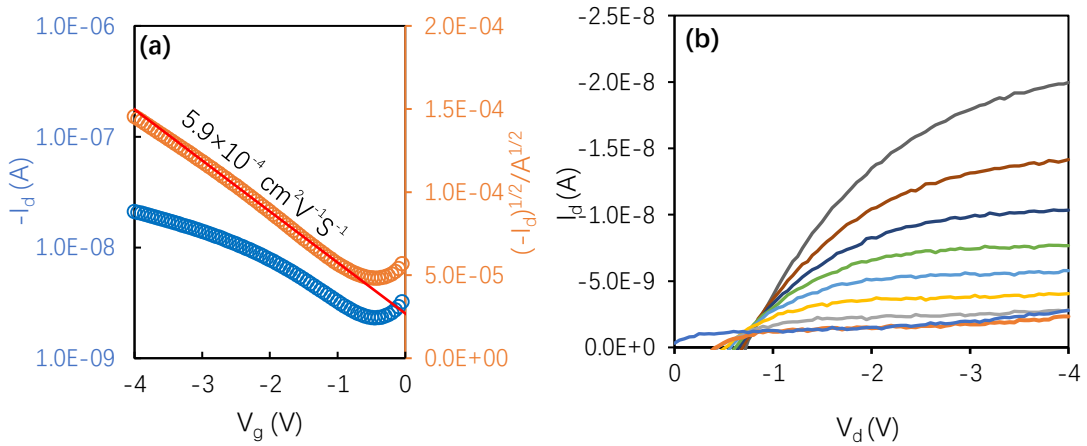

Figure S15 (a) Transfer I-V curves for a typical OFET of **1&3** (1:1) with a channel of 50 μm (L)×1 mm (W) as tested in air; (b) output I-V curves of the same OFET of **1&3** (1:1) with the gate voltage varied from 0 to −4V in −0.5 V steps.

4. Fabrication and testing of OFET-based gas sensors

(1) Monolayer OFET-based gas sensors and the gas sensing setup

Dip coated films were placed in vacuum at room temperature for 3 h to remove the solvent residue. Top contact drain and source electrodes (30 nm) were formed by vacuum-deposition of gold (30 nm thick) through a shadow mask onto the organic films using an Edward Auto 306 vacuum coating system with a Turbomolecular pump at a pressure of 4.0 × 10−6 torr or lower, with a deposition rate of ca. 2 nm/min to a thickness about 30 nm as measured by a quartz crystal sensor. The resulting interdigitated conducting channels were 3 mm (W)×60 μm (L)×14 channel.

As shown in Figure S16, the device was placed in a 1-liter chamber containing N_2, and gate, drain and source electrodes were led outside the chamber via gold wires and connected to a Keithley 4200 Semiconductor Characterization System. A flow of N_2 (1 L/min) containing analyte (NH_3 , NO_2 or organic vapor) of different concentrations was introduced. NH_3 gas and NO_2 gas of different concentration was obtained by diluting commercially available 100 ppm NH_3 or 100 ppm NO_2 in N_2 (Scientific Gas Engineering Co.,Ltd.) with pure N_2. As shown in Figure S17, organic vapors (hexylamine, diisopropylamine, triethylamine, etc.) were obtained by bubbling liquid compound to generate saturated vapor and then diluting to target concentration.[5]

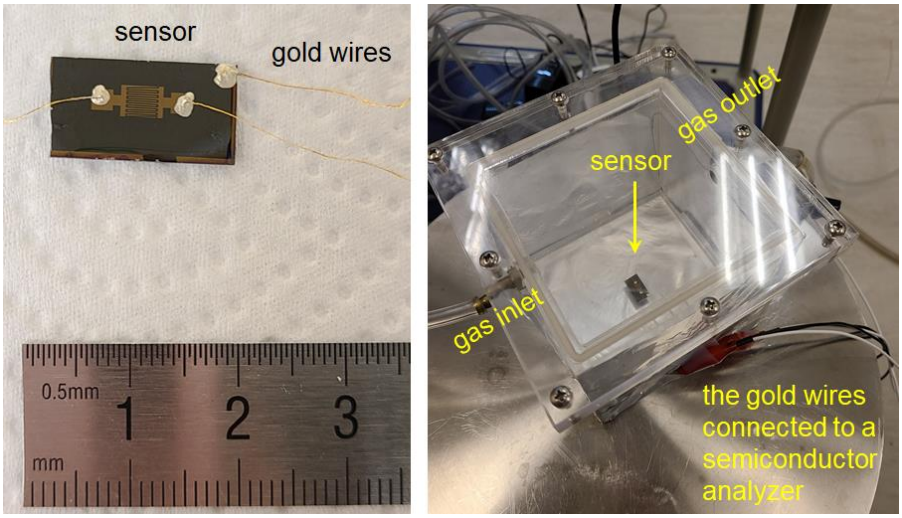

Figure S16 Pictures of the sensor and the gas sensing setup.

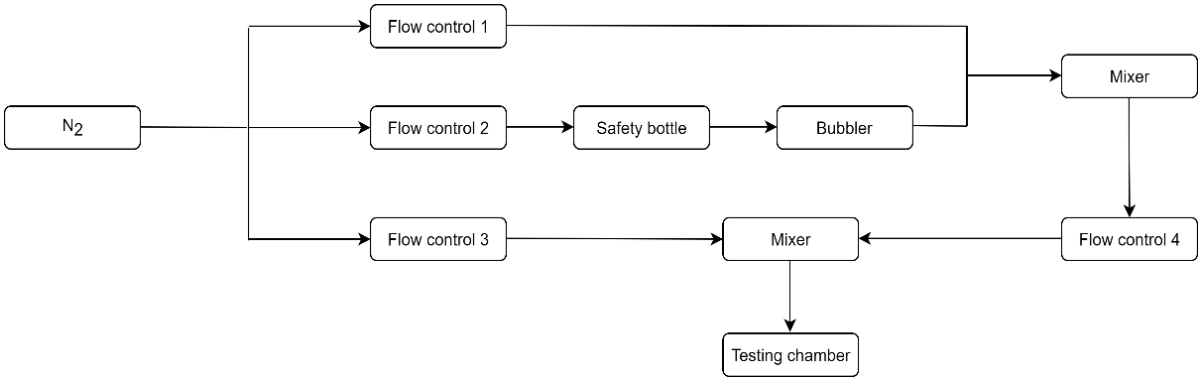

Figure S17 Schematic of gas generating and diluting process.

(2) Characterization of the OFET-based sensors for NH_3 and NO_2.

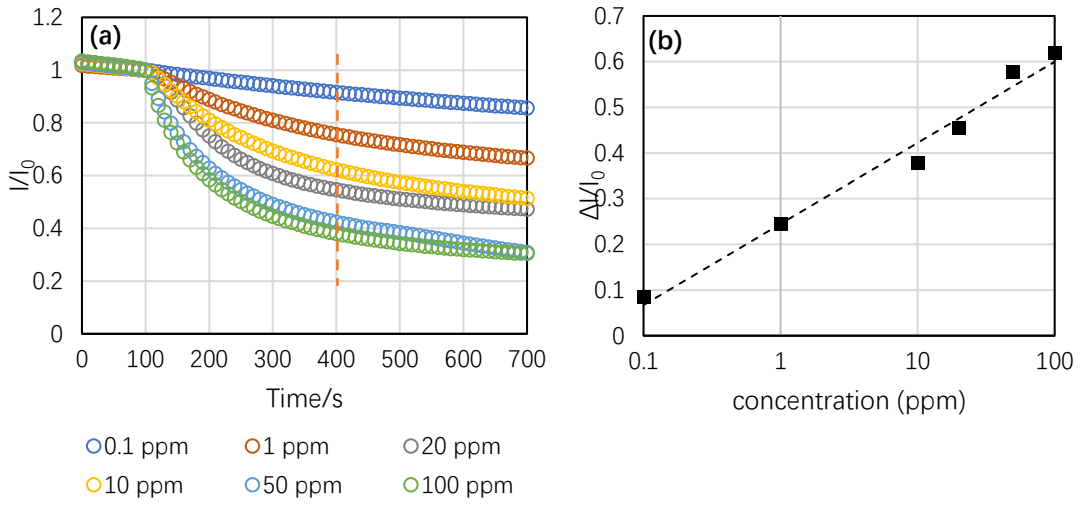

Figure S18 (a) Real-time change in the normalized drain current of the monolayer OFET of **1** in response to NH_3 of different concentrations (the drain and gate voltages both fixed at −2 V, and the OFET was exposed to NH_3 at the 100th second); (b) Change in the drain current of monolayer OFET of **1** after exposure to NH_3 for 300 s versus the concentration of NH_3.

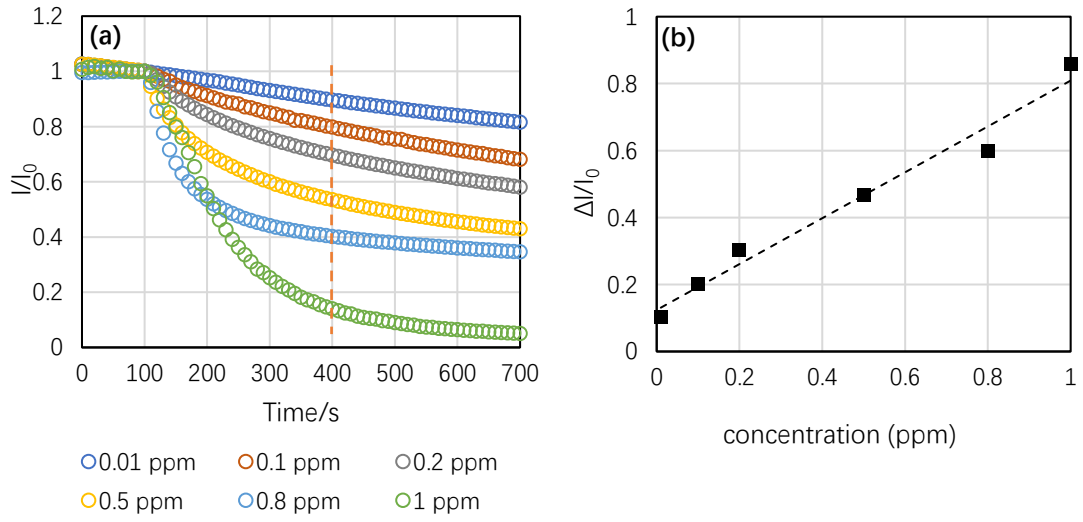

Figure S19 (a) Real-time change in the normalized drain current of the monolayer OFET of **1&2** (5:1) in response to NH_3 of different concentrations (the drain and gate voltages both fixed at −2 V, and the OFET was exposed to NH_3 at the 100th second); (b) change in the drain current of monolayer OFET of **1&2** (5:1) after exposure to NH_3 for 300 s versus the concentration of NH_3.

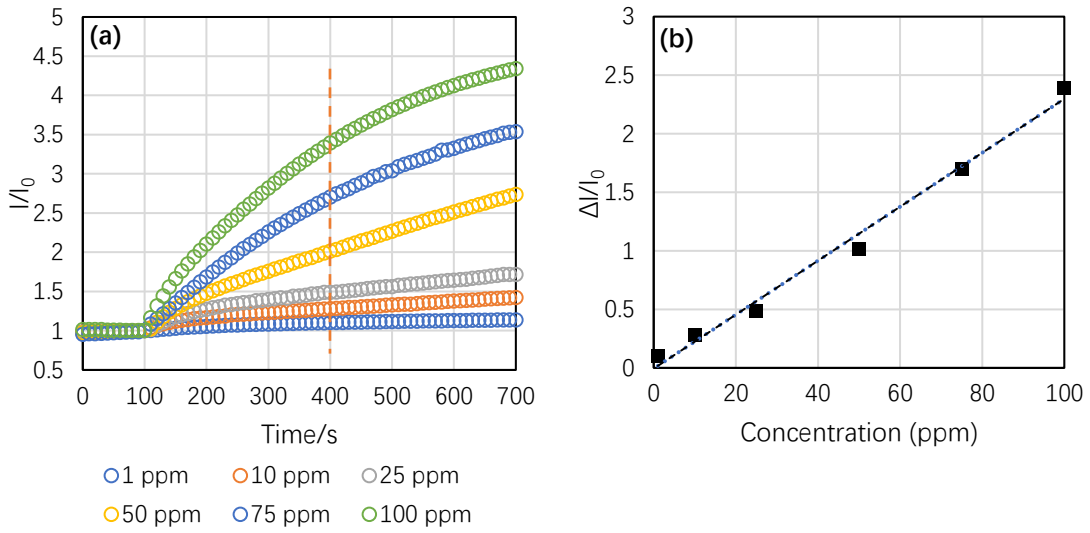

Figure S20 (a) Real-time change in the normalized drain current of the monolayer OFET of **1**&**3** (1:1) in response to NO_2 of different concentrations (the drain and gate voltages both fixed at −2 V, and the OFET was exposed to NO_2 at the 100th second); (b) change in the drain current of monolayer OFET of **1**&**3** (1:1) after exposure to NO_2 for 300 s versus the concentration of NO_2.

5. Reference

1 L. Shan, D. Liu, H. Li, X. Xu, B. Shan, J.-B. Xu and Q. Miao, *Adv. Mater.*, 2015, **27**, 3418.

2 C. Li, H. Wu, T. Zhang, Y. Liang, B. Zheng, J. Xia, J. Xu and Q. Miao, *Chem*, 2018, **4**, 1416.

3. D. Liu, X. Xu, Y. Su, Z. He, J. Xu, Q. Miao, *Angew. Chem. Int. Ed.* 2013, **52**, 6222–6227.

4. The commonly used formal potential of the redox couple of ferrocenium/ferrocene (Fc+/Fc) in the Fermi scale is -5.1 eV, which is calculated on the basis of an approximation neglecting solvent effects using a work function of 4.46 eV for the normal hydrogen electrode (NHE) and an electrochemical potential of 0.64 V for (Fc+/Fc) versus NHE. See: C. M. Cardona, W. Li, A. E. Kaifer, D. Stockdale, G. C. Bazan, *Adv. Mater.* 2011, **23**, 2367–2371.

5. B. Liu, Y. Huang, K. WL. Kam, W.-F. Cheung, N. Zhao, B. Zheng, *Biosensors and Bioelectronics: X*, 2019, **1**, 100016.